

Modelling of diffraction and complex reflection properties by wave field extrapolation

Rob Opdam, Diemer de Vries, Michael Vorländer

Institute of Technical Acoustics, RWTH Aachen University, 52066 Aachen, Germany

e-mail: rob.opdam@akustik.rwth-aachen.de

Introduction

To be able to investigate the effect of non-locally reacting boundaries on a sound field, a boundary element method is proposed, which is able to simulate such effects. This method is derived from a in seismic exploration widely known WRW model [1]. The model is similar to boundary element methods (BEM) where the Kirchhoff-Helmholtz integral is solved. The difference is that with the WRW model the Rayleigh-II integral is solved. This simplifies the calculation such that it is only necessary to know the pressure at the integral boundary instead of the pressure and the normal velocity, like for the Kirchhoff-Helmholtz integral. A more important result is that the use of the Rayleigh-II integral can be easily transcribed in matrix multiplications that represent spatial convolutions [1], which gives ample insight in the physical process of non-locally reacting boundaries [2]. The non-locally reacting boundaries can be translated in an angle dependent reflection coefficient. The implementation of the angle dependency in the WRW model will be explained here briefly. A more complete overview of the model for enclosed spaces is given in [3, 4].

WRW model

The WRW model is based on wave field extrapolation using the Rayleigh-II integral:

$$P(\vec{r}_A, \omega) = \frac{jk}{2\pi} \int_S \left[P(\vec{r}_S, \omega) \frac{1 + jk\Delta r}{\Delta r} \cos(\phi) \frac{e^{-jk\Delta r}}{\Delta r} \right] dS \quad (1)$$

where $\Delta r = |\vec{\Delta r}| = |\vec{r}_A - \vec{r}_S|$ is the distance from a secondary source point on the boundary S and the reconstruction point A within an enclosed volume, ϕ is the angle between the normal vector \vec{n} pointing inward to the volume and the vector $\vec{\Delta r}$ between a secondary source and the reconstruction point, P the pressure and wavenumber k is defined as the angular frequency ω divided by the propagation velocity c . The reflected pressure field can then be written as a discretised representation of the Rayleigh-II integral and given by:

$$\vec{P}(z_d) = [\mathbf{W}(z_d, z_b) \mathbf{R}(z_b) \mathbf{W}(z_b, z_s)] \vec{S}(z_s) \quad (2)$$

here are $\vec{P}(z_d)$ the vector with resulting pressures at the detectors in plane z_d , $\vec{S}(z_s)$ the vector containing the source properties, $\mathbf{W}(z_b, z_s)$ the matrix containing propagation kernels from the sources at z_s to the boundary at z_b , in the same way for $\mathbf{W}(z_d, z_b)$ from the boundary at z_b to the detectors at z_d and $\mathbf{R}(z_b)$ the matrix containing the reflective properties of the boundary at z_b . A schematic representation of the model is shown in Figure 1. For locally reacting boundaries the reflection

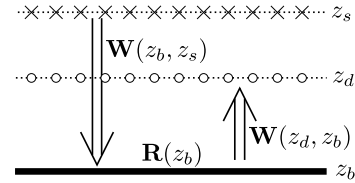


Figure 1: Propagation from sources (\times) to boundary to detectors (\circ).

matrix $\mathbf{R}(z_b)$ is defined as a diagonal matrix with all zeros and on the diagonal the (complex) reflection factor for each discretised point on the boundary. Each row in this matrix can be seen as a reflectivity convolution operator and for a locally reacting boundary this convolution operator is represented by a finite impulse in the space-frequency domain as shown on the left in Figure 2. Transforming this into the wavenumber-frequency domain by applying a spatial Fourier transform, where $k_x = \frac{\omega}{c} \sin \alpha$ (with α the angle of incidence), this gives a unity response as given on the right in Figure 2. This

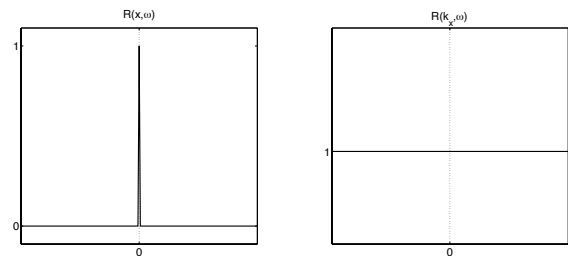


Figure 2: Locally reacting reflection in space-frequency $R(x, \omega)$ and wavenumber-frequency $R(k_x, \omega)$ domain.

spatial Fourier transformation can be used to define an angle dependent reflectivity behaviour of a boundary in the wavenumber-frequency domain and transform this into the space-frequency domain. In Figure 3 this is applied for the case that small angles of incidence are fully reflected and outside there is no reflection at all. The

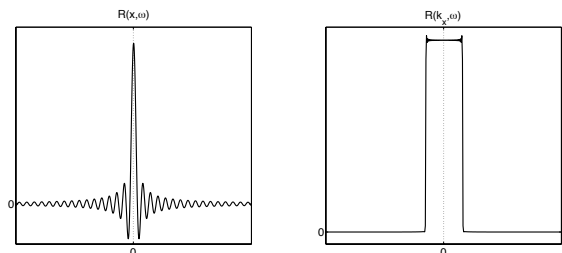


Figure 3: Non-locally reacting reflection in space-frequency $R(x, \omega)$ and wavenumber-frequency $R(k_x, \omega)$ domain.

reflection matrix will be defined for the non-locally re-

flective case as:

$$\mathbf{R}_b = \begin{pmatrix} R(x_{11}, \omega) & R(x_{12}, \omega) & \cdots & 0 \\ R(x_{21}, \omega) & R(x_{22}, \omega) & & \\ \vdots & & \ddots & \vdots \\ 0 & & \cdots & R(x_{NN}, \omega) \end{pmatrix}. \quad (3)$$

The off diagonal values represent the influence of the neighbouring points on the point at the diagonal. This extreme example for the reflectivity, as given in Figure 3, will be used in two examples to show the influence on the total reflected pressure field.

Results

Two geometries are used to show the difference between a locally and non-locally reacting boundary property. For the locally reacting case the reflectivity function from Figure 2 is used and for the non-locally the one of Figure 3. The first geometry is a simple wall with two source positions, shown in Figure 4. The time domain result of

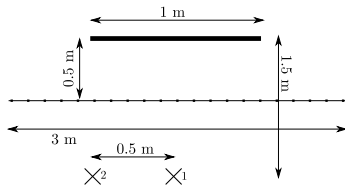


Figure 4: Wall geometry with two source positions and detector array.

the reflected pressure field is given in Figure 5. Top figure gives the result for source position 1 and the bottom figure the result for source position 2. The second geome-

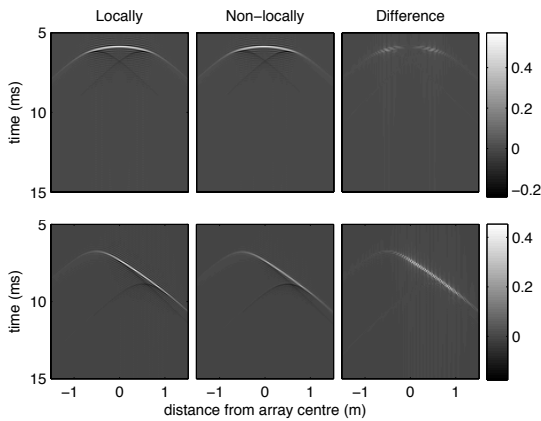


Figure 5: Reflected pressure fields (in Pa) of non-locally and locally reacting wall, and the difference. For source position 1 (top figure) and 2 (bottom figure).

try is an L-shaped wall with in front a single point source and a detector array as shown in Figure 6. The resulting reflected pressure field shows the edge diffraction of the wall ends (arrow a), first order reflection of the wall parallel to the detector array (arrow b) and the second order reflection of the sidewall to the parallel wall (arrow c), as shown in Figure 7. The first reflection does not show much difference, because the incoming wave field is

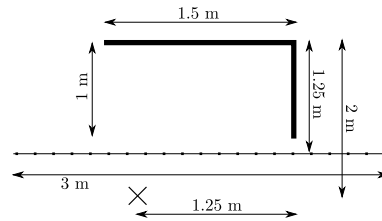


Figure 6: Geometry L-wall with source and detector array.

in an almost perpendicular angle. So it reacts as a quasi locally reacting surface due to the defined reflection coefficient function. On the other hand the second order reflection is a result of a wave field coming in under an angle. This explains the difference between the second order reflection and the first order reflection. Of course a block function for the reflectivity is an extreme case, in real materials the difference will be less.

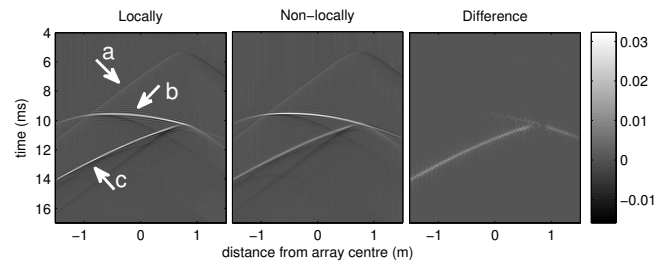


Figure 7: Reflected pressure fields (in Pa) of non-locally and locally reacting L-wall, and the difference.

Conclusions

The WRW model has been used to implement complex, frequency dependent and non-locally reacting boundary conditions, which results in an angle dependent reflectivity. It has been shown for an extreme case that the angle dependent reflection properties of boundaries are of importance to describe the reflected pressure field. Further research will involve the complete modelling of a room and assess the differences in the room acoustical parameters by using locally and non-locally reacting assumptions of the boundaries.

References

- [1] A.J. Berkhout, "Applied Seismic Wave Theory", *Elsevier, Amsterdam, 1987*
- [2] C.G.M. de Bruin, C.P.A. Wapenaar, A.J. Berkhout, "Angle-dependent reflectivity by means of prestack migration", *Geophysics* **55**(9), 1223-1234 (1990)
- [3] A.J. Berkhout, D. de Vries, J. Baan, B.W. van den Oetelaar, "A wave field extrapolation approach to acoustical modeling in enclosed spaces", *J. Acoust. Soc. Am.* **105**(3), 1725-1733 (1999)
- [4] R.C.G. Opdam, D. de Vries, M. Vorländer, "Wave based modelling of enclosed spaces by a sequence of matrix multiplications", *Proceedings Acoustics 2012, Nantes*